

Satellite-Induced Multipath Analysis on the Cause of BeiDou Code Pseudorange Bias

Hailong Xu, Xiaowei Cui and Mingquan Lu

Abstract Data from previous observation have shown that the BeiDou satellite navigation system (BDS) has been suffering from satellite-induced elevation-dependent code pseudorange bias, which can be as much as 1 m and degrade the performance of high-precision applications such as Precise Point Positioning (PPP). Mechanism analysis on the cause of the bias has been absent in previous literature, which is essential to avoid the issue from happening again in following satellites. In this paper, both theoretical analyses and simulations are performed, proving that the bias can be caused by the multipath effect induced by the transmitting array on the satellite. Based on a proper model of this satellite-induced multipath effect, the bias values can be calculated through mathematical derivation. Under certain model parameters, the simulation results agree with the observed bias values very well. Methods and conclusions of this paper are useful in both investigating the current BeiDou bias issue and the process of design, development and test of following satellites by satellite manufactures.

Keywords BeiDou satellite navigation system · High-precision application, precise point positioning · Code pseudorange bias · Satellite-induced multipath · Correlation function

1 Introduction

With the system construction advancing and the application areas expanding, the BeiDou satellite navigation system (BDS) is becoming more and more important in both military and civilian fields. All of this is based on the condition that the system provides code pseudorange measure precise enough to end receivers. However, through the transmitting, propagating and receiving processes of the navigation signals, it is inevitable that biases will be induced to the pseudorange

H. Xu · X. Cui (✉) · M. Lu

Department of Electronic Engineering, Tsinghua University, Beijing, China
e-mail: cxw2005@mail.tsinghua.edu.cn

© Springer Nature Singapore Pte Ltd. 2017

J. Sun et al. (eds.), *China Satellite Navigation Conference (CSNC) 2017*

Proceedings: Volume II, Lecture Notes in Electrical Engineering 438,

DOI 10.1007/978-981-10-4591-2_2

measurements. The bias sources include the satellite clock and orbit error, the ionosphere and troposphere delay, as well as the multipath effect on the receiver end. Features and correcting methods of these biases have been studied extensively in the past. However, in recent years, a new kind of pseudorange bias is observed in BDS, whose values are dependent on the elevation of the satellite from the view of the receiver and can be as large as 1 m. This bias is independent of the type, location, observation interval of the receiver, but holds differences between the two satellite groups, which are in medium earth orbits (MEO) and inclined geostationary orbits (IGSO), respectively, thus is supposed to be caused by the satellites [1]. This bias has little effect on absolute positioning applications due to the limited accuracy requirements, but can degrade the performance of some high-precision applications using code pseudorange measurements but without differencing techniques, such as Precise Point Positioning (PPP), thus restricts the application extension of the system.

Towards this issue, one countermeasure is to determine the bias values under different satellite elevations from historical observations, then perform compensation in the receiver [1]. Another countermeasure is to adjust the broadcasted ephemeris, and use the orbit shift calculated from the ephemeris with respect to the true orbit to counteract the bias [2]. However, these solutions cannot eliminate the bias from the source. To solve the issue thoroughly, the cause of the bias must be found, and then be avoided strictly in the design and manufacture of following satellites.

This paper proves through theoretical analyses and simulations that, signal delays between different elements of the satellite antenna can cause bias similar to the observed one. These delays can be modelled as the satellite-induced multipath effect, in which the direct and multipath signals result in their respective correlation functions with different delays in the receiver, causing the peak of the composite correlation function to be distorted. Based on an accurate model of the satellite-induced multipath effect, the bias values can be calculated through mathematical derivation. Under certain parameters of the model, the simulated bias agree with the observed one very well. The methods and conclusions of this paper are helpful in the investigation of the BeiDou bias issue, as well as in the design, development and test of the following satellites by satellite manufactures.

2 Transmitting Array Modelling

Navigation satellites transmit signals towards the earth from orbits of certain altitudes, just as presented in Fig. 1. The off-boresight angle is defined as the angle between the line from the satellite to the earth center and the line from the satellite to the receiver. For a receiver on the earth's surface, the larger the satellite elevation, the smaller the off-boresight angle, and so is the distance between the satellite and the receiver. Thus, the propagation loss of the signal increases with the off-boresight angle. In order to let the signal reach the earth's surface with nearly

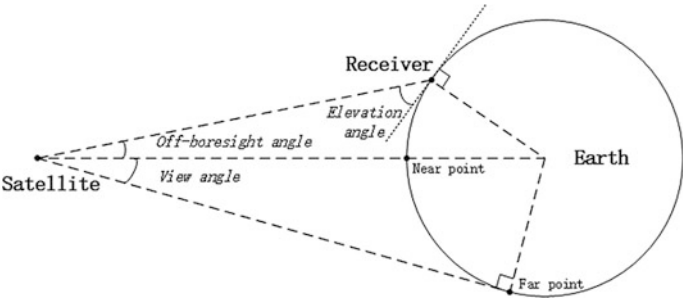
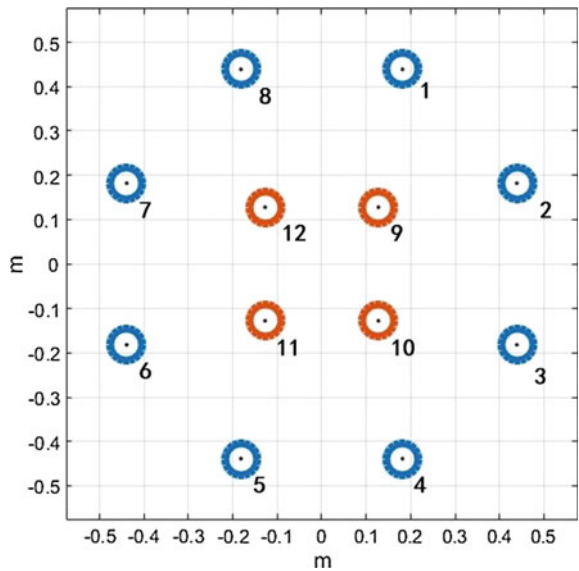


Fig. 1 Geometrical relationship of the satellite, the earth and the receiver

Fig. 2 Geometry of the GPS Block IIR transmitting array



equal power, the beam pattern of the transmitting antenna on the satellite should be shaped to form a dimple towards the earth's center [3].

In order to achieve this goal, multi-antenna arrays are used to transmit signals on the satellites [3, 4]. For example, Fig. 2 presents the array geometry of the GPS Block IIR satellite, including 8 equally distributed elements in the outer ring and 4 equally distributed elements in the inner ring [3]. The signal transmitting flow on the satellite is presented in Fig. 3. For beam pattern shaping, the navigation signal of a particular frequency is generated by the signal generation payload before being divided into 12 streams by the power dividing and phase shifting network, each of which is transferred to one array element to be transmitted. In the division, most of the power is allocated to the inner ring, forming a strong wide beam, while the rest is allocated to the outer ring, forming a weak narrow beam. Besides, the carrier

Fig. 3 Signal transmitting flow on the satellite

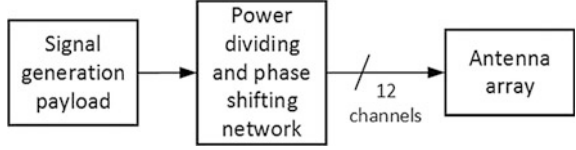


Table 1 BeiDou MEO satellite transmitting array parameters used in this paper

Parameters	Values
Radius of inner ring r_{inner}	18.03 cm
Radius of outer ring r_{outer}	47.50 cm
Power allocation of inner ring P_{inner}	95%
Power allocation of outer ring P_{outer}	5%
Phase shift of inner ring ϕ_{inner}	0°
Phase shift of outer ring ϕ_{outer}	180°

phase of the signal transmitted by the outer ring is shifted by 180° with respect to the inner ring. Thus, the composite beam pattern is obtained by subtracting the narrow beam from the wide beam, with a dimple towards the earth's center being formed.

The parameters of the BeiDou satellite transmitting antenna are not available in open literature, so it is assumed in this paper the BeiDou MEO satellite has an array with similar geometry and parameters with the GPS Block IIR satellite. Through a “try and see” method, it concludes that under the parameters presented in Table 1, the desired beam pattern can be obtained approximately. Based on these parameters, the weighting value corresponding to each element can be calculated by following equations:

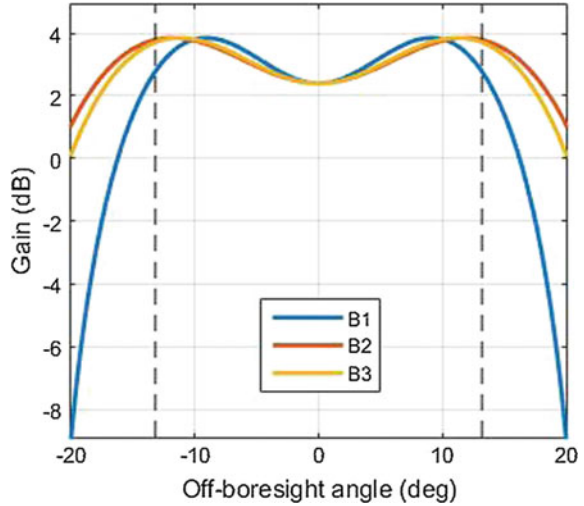
$$w_{outer} = -\sqrt{P_{outer}/8}, \quad w_{inner} = \sqrt{P_{inner}/4}. \quad (1)$$

Then, under the isotropic element assumption, the transfer function of the array can be written by [5]

$$H(f, \theta) = \sum_{i=1}^{12} w_i e^{-j\frac{2\pi}{\lambda} \mathbf{p}_i \cdot \mathbf{a}(\theta)}, \quad (2)$$

where f denotes the frequency, λ denotes the corresponding wavelength, and θ denotes the off-boresight angle. Due to the rotational symmetry of the array geometry, the beam pattern variations along the same off-boresight angle are omitted. Index i ranging from 1 to 8 corresponds to the outer ring with $w_i = w_{outer}$, while index i ranging from 9 to 12 corresponds to the inner ring with $w_i = w_{inner}$. Vector \mathbf{p}_i denotes the position of the i th element, and vector $\mathbf{a}(\theta)$ denotes the signal transmitting direction. Fixing f to be B1 (1561.098 MHz), B2 (1207.14 MHz) and B3 (1268.52 MHz), respectively, the beam pattern of the three frequencies can be

Fig. 4 Simulated beam patterns of the BeiDou MEO satellite transmitting array antenna. The *dotted lines* depict the view angle of the satellite towards the earth



obtained, which are presented in Fig. 4. It can be seen that the desired dimples are indeed formed, the depths of which are nearly identical to the propagation loss differences between the near point and far point in Fig. 1, proving the rationality of the parameters used. Following simulations will be performed under these parameters.

3 Satellite-Induced Multipath and Pseudorange Bias

In practice non-ideal factors always exist in the power dividing and phase shifting network depicted in Fig. 3, which can cause signal transfer delays between the different elements. These delays can be modeled as the satellite-induced multipath effect. Considering the two-ring array geometry, it is reasonable to assume that there is no delay difference between the elements within the same ring, but the signal transmitted by the outer ring is delayed by τ_d with respect to the inner ring. Thus, the signal out of the inner ring can be regarded as the direct path signal, while the signal out of the outer ring can be regarded as the multipath signal. The complex envelopes of them can be written as follows, respectively:

$$\tilde{s}_{inner}(t) = d(t)c(t)e^{j\phi_{inner}}, \quad (3)$$

$$\tilde{s}_{outer}(t) = \alpha d(t - \tau_d)c(t - \tau_d)e^{j\phi_{outer}}, \quad (4)$$

where $d(t)$ denotes the ephemeris bits, $c(t)$ denotes the pseudo-random ranging codes, ϕ_{inner} and ϕ_{outer} denote the carrier phases of the direct and the multipath signals, respectively, while α denotes the amplitude ratio of the multipath signal to

the direct signal. Assuming that within the observation interval, the ephemeris bit of the two signals are the same, then the complex envelope of the composite signal is given by

$$\tilde{s}(t) \approx d(t)(c(t) + \alpha c(t - \tau_d) e^{j\Delta\phi}) e^{j\phi_{inner}}, \quad (5)$$

where

$$\Delta\phi = \phi_{outer} - \phi_{inner}. \quad (6)$$

At the receiver end, a delayed local code $c(t - \tau)$ is generated to correlate with the received signal, resulting in the correlation function to be

$$R'(\tau) = \|R(\tau) + \alpha e^{j\Delta\phi} R(\tau - \tau_d)\|_2, \quad (7)$$

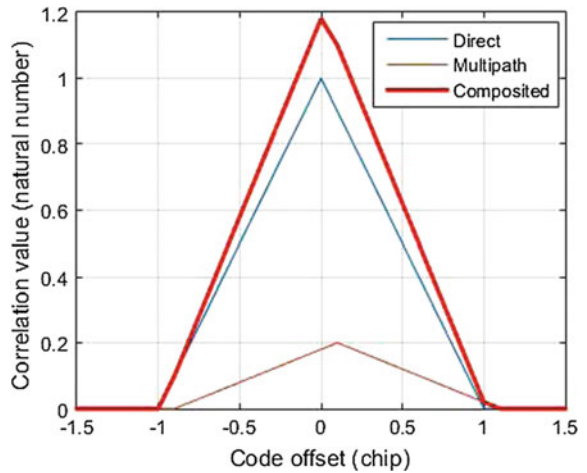
where $\|\cdot\|_2$ denotes the 2-norm operation, and $R(\tau)$ is the ideal correlation function of the pseudo-random ranging codes which is given by

$$R(\tau) = \begin{cases} (1 - |\frac{\tau}{T_c}|), & |\tau| \leq T_c \\ 0, & |\tau| > T_c \end{cases}, \quad (8)$$

with T_c denoting the period of one code chip.

Figure 5 presents an instance of the correlation functions of the direct, multipath and composite signals when $\Delta\phi$ equals zero. Although the ideal correlation function $R(\tau)$ is symmetric and reaches its peak at $\tau = 0$, the composite correlation function $R'(\tau)$ is no longer symmetric and suffers a peak shift. In a typical receiver the Delay-Lock-Loop (DLL) is usually used to estimate and track the code phase through finding the peak of the correlation function [6]. With D denoting the early-minus-late interval of the DLL, let

Fig. 5 An example of the direct, multipath and composite correlation functions



$$R'(\tau_e - D/2) = R'(\tau_e + D/2), \quad (9)$$

then τ_e is the code phase bias. As a result, the code pseudorange bias is calculated by

$$\rho_e = c \cdot \tau_e, \quad (1.10)$$

where c is the speed of light.

The amplitude ratio α can be calculated from the array model. For this purpose, Eq. (2) is divided into two parts for the two rings, respectively:

$$H_{outer}(f, \theta) = \sum_{i=1}^8 w_{outer} e^{-j \frac{2\pi}{\lambda_c} \mathbf{p}_i \mathbf{a}(\theta)}, \quad (11)$$

$$H_{inner}(f, \theta) = \sum_{i=9}^{12} w_{inner} e^{-j \frac{2\pi}{\lambda_c} \mathbf{p}_i \mathbf{a}(\theta)}. \quad (12)$$

Under the narrowband presumption [5], λ can be fixed to λ_c which is the wavelength at the central frequency of the signal, so the argument f can be omitted. If the center of the array geometry is at the antenna coordinate origin, then

$$\mathbf{p}_i = -\mathbf{p}_{i+4} (i = 1, 2, 3, 4), \quad \mathbf{p}_j = -\mathbf{p}_{j+2} (j = 9, 10). \quad (13)$$

Thus the transfer functions of the outer and inner rings can be reformed as

$$H_{outer}(\theta) = 2w_{outer} \sum_{i=1}^4 \cos\left(\frac{2\pi}{\lambda_c} \mathbf{p}_i \mathbf{a}(\theta)\right), \quad (14)$$

$$H_{inner}(\theta) = 2w_{inner} \sum_{i=9}^{10} \cos\left(\frac{2\pi}{\lambda_c} \mathbf{p}_i \mathbf{a}(\theta)\right). \quad (15)$$

Therefore, α is obtained by

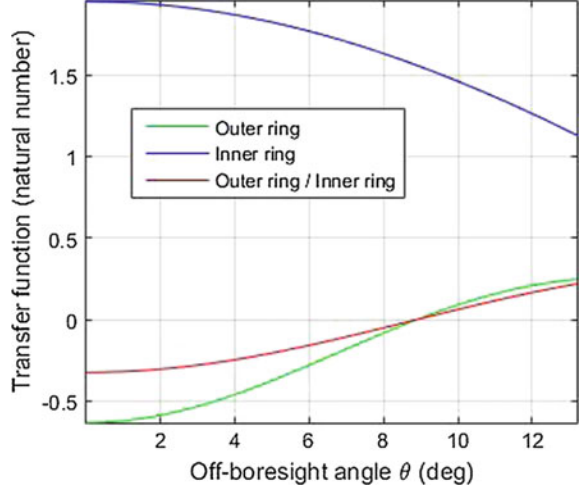
$$\alpha(\theta) = \frac{H_{outer}(\theta)}{H_{inner}(\theta)} \quad (16)$$

Figure 6 presents the transfer function variations of the inner and outer rings, as well as the amplitude ratio α over the off-boresight angle.

From equations from (7) to (1.10) it can be seen that the code pseudorange bias is determined by α , $\Delta\phi$ and τ_d . Parameter α is dependent on θ , while θ and the satellite elevation el are in one-to-one correspondence. Thus it concludes that the code pseudorange bias is dependent on the satellite elevation.

If α is small enough, then τ_e can be calculated by Braasch's approximate formula [7]:

Fig. 6 Transfer function variations over the off-boresight angle for the inner and outer rings of the transmitting antenna array



$$\tau_e = \begin{cases} \frac{\beta\tau_d}{\beta+1} & 0 \leq \tau_d \leq \frac{D}{2}(\beta+1) \\ \frac{\beta D}{2} & \frac{D}{2}(\beta+1) \leq \tau_d \leq T_c + \frac{D}{2}(\beta-1) \end{cases}, \quad (17)$$

with

$$\beta = \alpha \cos(\Delta\phi). \quad (18)$$

The chip period of the ranging code in BDS is usually hundreds of nanoseconds, while D is usually set to $T_c/2$ or a bit smaller. Besides, it is reasonable to assume τ_d is about tens of nanoseconds or less. Then, the condition of the first branch in Eq. (17) is always satisfied, leading the calculation formula to be

$$\rho_e(\theta) = c \cdot \frac{\alpha(\theta) \cos(\Delta\phi) \tau_d}{\alpha(\theta) \cos(\Delta\phi) + 1}. \quad (19)$$

After $\Delta\phi$ and τ_d are fixed, the code pseudorange bias under any elevation can be calculated using this equation.

4 Simulation

The B1 signal of BeiDou's MEO satellites is taken for example in this section, where simulation results of how the code pseudorange bias varies with the satellite elevation angle are given, and comparisons with the observed results given in [1] are made. The goal is to find proper parameter combinations in the parameter

domain of $\Delta\phi$ and τ_d , with which the simulated bias values agree with the observations very well.

Here we define a parameter called the bias dynamic as below

$$\Delta\rho_e = \rho_e|_{el=0^\circ} - \rho_e|_{el=90^\circ} \quad (20)$$

When the simulated and observed $\Delta\rho_e$ are the same, then it is highly possible that the simulated and observed bias values are very close to each other for each satellite elevations.

Figure 7 presents how $\Delta\rho_e$ varies with τ_d , with the observed $\Delta\rho_e$ depicted by the dotted red line. It can be seen that under different values of $\Delta\phi$, the “proper” values of τ_d under which the simulated and observed $\Delta\rho_e$ meet are also different. As a step further, Fig. 8 presents how the proper values of τ_d vary with $\Delta\phi$. Considering the even symmetry of $\cos(\Delta\phi)$ in Eq. (19) and assuming τ_d is positive, only the interval $0 \leq \Delta\phi < \pi/2$ needs to be considered. It can be seen that the proper τ_d increases with $\Delta\phi$. When $\Delta\phi$ is zero, τ_d achieves the minimum, which is 7.69 ns.

In the end, Fig. 9 presents how the code pseudorange bias varies over the satellite elevation under a few randomly selected parameter combinations on the curve of Fig. 8. It can be seen that under all these parameter combinations, the simulated results agree with the observations very well. Similar results can be obtained for the B1 and B2 signals of the BeiDou MEO satellite, as well as the B1, B2 and B3 signals of the BeiDou IGSO satellite, thus proving the effectiveness of the method proposed in this paper.

It is worth emphasizing that, due to the real parameters of the BeiDou satellite transmitting antennas are not available in open literature, the parameters of GPS Block IIR satellite are used as demonstration in this paper’s simulations. Although with this compromise, the results are still persuasive enough to illustrate the

Fig. 7 Code pseudorange bias dynamic variations over the multipath signal delay

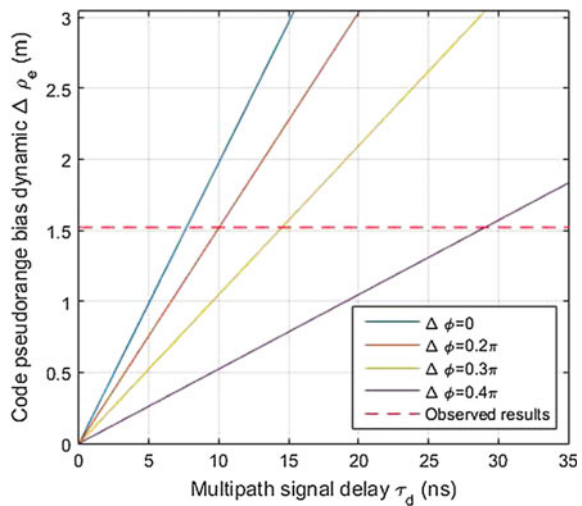


Fig. 8 Multipath signal delay variations over the phase difference between the direct and multipath signals

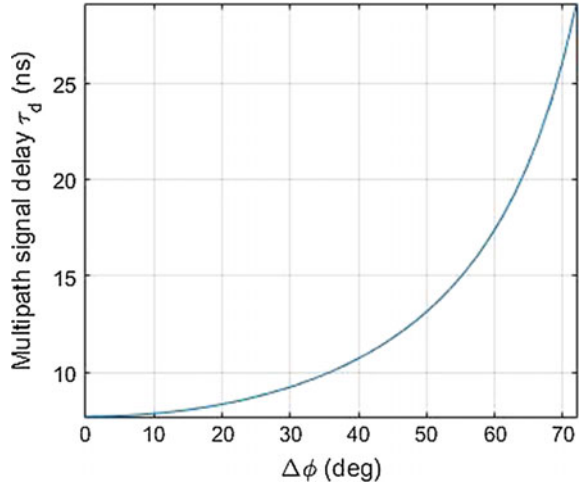
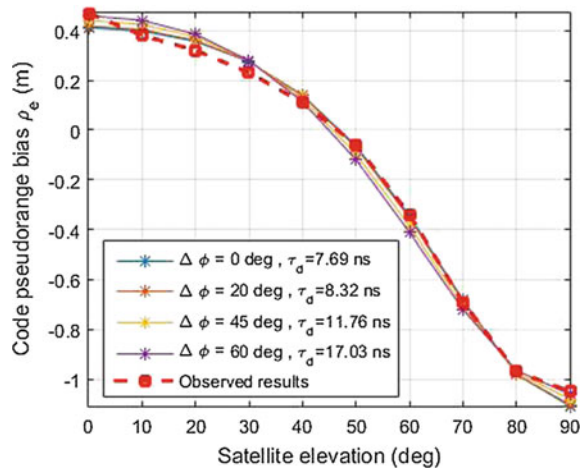


Fig. 9 Simulated code pseudorange bias variations over the satellite elevation



principle. Once the real parameters are given, more accurate simulation results can be obtained using the same method given above.

5 Conclusion

In order to analyse the cause of the code pseudorange bias anomaly of the BeiDou system, this paper models the satellite-induced multipath effect and proposes a method of calculating the bias value. Simulation results prove that transfer delays between different antenna elements can indeed cause elevation-dependent code

pseudorange bias, and under certain parameter combinations of the multipath model, simulated results agree with the observations very well. Therefore, it concludes that the anomaly may be caused by the satellite-induced multipath effect. Accordingly, we suggest that in the investigation of the BeiDou bias anomaly, special attention should be paid to see if the transfer delays motioned above exist. In addition, in order to avoid the satellite-induced multipath effect in the manufacture of following satellites, the transfer delay inconsistency of different antenna elements should be strictly restricted in the design, development and test processes.

References

1. Wanninger L, Beer S (2015) BeiDou satellite-induced code pseudorange variations: diagnosis and therapy. *GPS Solutions* 19:639–648
2. Springer T, Dilssner F (2009) SVN49 and other GPS anomalies. *Inside GNSS* 2009:32–36
3. Parkinson B, Spilker J (1996) *Global position system: theory and applications*, vol 1. AIAA, New York, pp 234–239
4. Marquis A, Reigh L (2015) The GPS block IIR and IIR-M broadcast L-band antenna panel: its pattern and performance. *Navigation* 62(4):329–347
5. Trees V (2002) *Optimum array processing: Part IV of detection, estimation and modulation theory*. Wiley, New York
6. Enge P (2001) *The global positioning system: signals, measurements, and performance*. Ganga-Jamuna Press, Lincoln, Massachusetts
7. Braasch S, Dibenedetto F (2001) Spread-spectrum ranging multipath model validation. *IEEE Trans Aerosp Electron Syst* 37(1):298–304

China Satellite Navigation Conference (CSNC) 2017

Proceedings: Volume II

Sun, J.; Liu, J.; Yang, Y.; Fan, S.; Yu, W. (Eds.)

2017, XIX, 647 p. 347 illus., Hardcover

ISBN: 978-981-10-4590-5